

# Dynamics and Control of Resistive Wall Modes with Magnetic Feedback Control Coils: Experiment and Theory

M. E. Mauel, J. Bialek, A. H. Boozer, C. Cates, R. James, O. Katsuro-Hopkins, A. Klein, Y. Liu, D. A. Maurer, D. Maslovsky, G. A. Navratil, T. S. Pedersen, M. Shilov, and N. Stillits

Department of Applied Physics and Applied Mathematics  
Columbia University, New York, NY 10027, USA

e-mail contact of main author: mauel@columbia.edu

**Abstract.** Fundamental theory, experimental observations, and modeling of resistive wall mode (RWM) dynamics and active feedback control are reported. In the RWM, the plasma responds to and interacts with external current-carrying conductors. Although this response is complex, it is still possible to construct simple but accurate models for kink dynamics by combining separate determinations for the external currents, using the VALEN code, and for the plasma's inductance matrix, using an MHD code such as DCON. These computations have been performed for wall-stabilized kink modes in the HBT-EP device, and they illustrate a remarkable feature of the theory: when the plasma's inductance matrix is dominated by a single eigenmode and when the surrounding current-carrying structures are properly characterized, then the resonant kink response is represented by a small number of parameters. In HBT-EP, RWM dynamics are studied by programming quasi-static and rapid “phase-flip” changes of the external magnetic perturbation and directly measuring the plasma response as a function of kink stability and plasma rotation. The response evolves in time, is easily measured, and involves excitation of both the wall-stabilized kink and the RWM. High-speed, active feedback control of the RWM using VALEN-optimized mode control techniques and high-throughput digital processors is also reported. Using newly-installed control coils that directly couple to the plasma surface, experiments demonstrate feedback mode suppression in rapidly rotating plasmas near the ideal wall stability limit.

## 1. Introduction

Among fusion's significant accomplishments during the past decade is the improved understanding and control of long-wavelength kink instabilities that grow on the rate of resistive penetration of a nearby conducting wall,  $\gamma_w$ . These slowly growing instabilities, called resistive wall modes (RWM), appear when nonaxisymmetric eddy currents in the wall oppose, or wall-stabilize, fast ideal kink modes. When the RWM is controlled, tokamaks and spherical tori can operate with high plasma pressure making possible advanced steady-state operating scenarios having good confinement and low current drive power requirements [1]. Stabilization of the RWM has been seen in tokamak experiments through sustained plasma rotation [2] or by active feedback control [3, 4]. Using the 3D electromagnetic modeling code VALEN [5], experiments have been realistically modeled, theoretical predictions have been benchmarked, and advanced control systems have been designed for several toroidal devices including HBT-EP [6], DIII-D, NSTX, JT-60SC, FIRE, and ITER. Although tremendous progress has been made, important questions remain concerning the physics

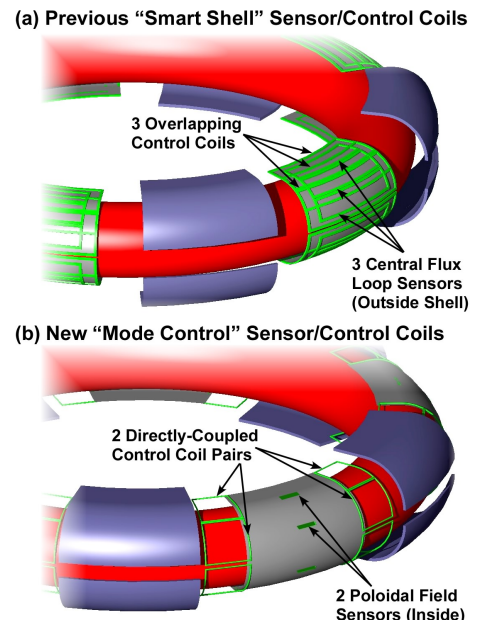


FIG. 1. Schematic of the HBT-EP (a) “smart-shell” and (b) “mode-control” sensor and control coils.

of plasma dissipation, the torque applied between the RWM and the external conductors, the dynamics of wall-stabilized kink modes, and the development of practical techniques that insure robust feedback control of the RWM [7].

This paper begins with a presentation of the fundamental theory behind the VALEN code and describes a general eigenmode procedure that can be used to implement optimized feedback systems for the RWM. Quantitative modeling requires (i) accurate information about the inductive coupling between current carrying structures and coils that lie outside the plasma and (ii) the equivalent currents on the plasma surface that represent the normal field of the perturbed plasma response,  $\delta B_n$ .

These quantitative models provide an useful interpretation of HBT-EP experiments. The HBT-EP tokamak was specially designed for systematic investigation of the effects of wall position and conductivity on kink mode stabilization and for the testing of sensor and control coil configurations for active control. Previous HBT-EP experiments demonstrated passive stabilization [8], observed the extent of mode structure variation with wall configuration, and directly measured the stabilizing eddy-currents [9]. The RWM instability was excited in HBT-EP when alternating segments of the previous HBT-EP wall were replaced with thin, more resistive wall segments [3]. RWM modes are also excited in stable plasma when control coil currents are programmed to resonate with the relatively simple eigenmodes observed in HBT-EP discharges [10]. We find the magnitude and phase of the observed resonant error field amplification implies a high torque parameter,  $\alpha \sim 1$ , that is fundamentally proportional to plasma dissipation [14] and defines the so-called “high dissipation” regime of RWM dynamics [15, 16]. This same parameterization also explains the observed dynamical response that follows a rapid “phase-flip” change of the external control coils [10]. Finally, using newly installed sensors and control coils (Fig. 1) that implement “optimized mode-control” feedback [6], we report the suppression of wall-stabilized kink modes in rapidly rotating plasma near the ideal wall stability limit.

## 2. Fundamental Theory

The response of a plasma to externally driven magnetic perturbations is an important topic in its own right and an essential element in the theory of resistive wall modes. Computational studies require not only the determination of the plasma response to external magnetic perturbations but also the inductive response of external conductors. Fortunately the calculation of these two responses can be separated. The separation arises from the magnetic interaction between the plasma and the external conductors being transmitted by a divergence and curl free magnetic field. In other words, the interaction field,  $\delta \vec{B}$ , is transmitted through the annular region surrounding the plasma by a solution to Laplace’s equation,  $\nabla^2 \phi = 0$  with  $\delta \vec{B} = \vec{\nabla} \phi$ .

The theory of Laplace’s equation implies that all of the magnetic effects of a plasma on the external world are given by the change in the tangential magnetic field at the

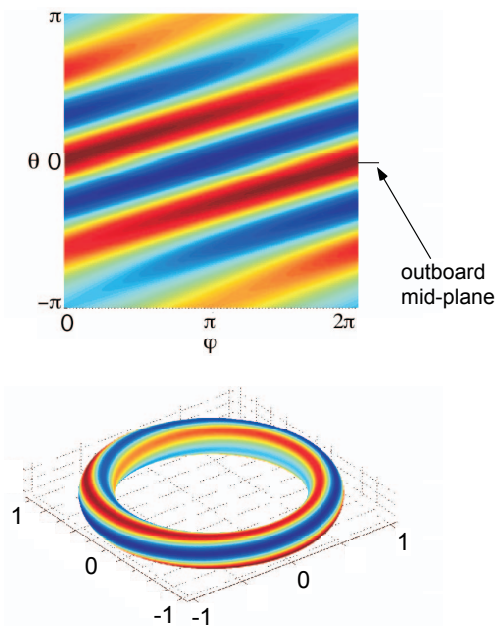


FIG. 2. The amplitude of the first expansion function,  $f_1(\theta, \varphi)$ , corresponding to the unstable plasma mode.

plasma surface that arises in response to a perturbation in the normal magnetic field. The tangential components of  $\delta\vec{B} = \vec{\nabla}\phi$  determine  $\phi$  on the surface while the normal component of  $\delta\vec{B}$  determines  $\hat{n} \cdot \vec{\nabla}\phi$ . If both  $\phi$  and  $\hat{n} \cdot \vec{\nabla}\phi$  are known on the plasma surface, then the theory of Laplace's equation says that one can obtain a unique answer for the magnetic field due to the currents in the plasma,  $\delta\vec{B}_p(\vec{x})$ , throughout the region external to the plasma.

This property of Laplace's equation is illustrated by a cylindrical model of the plasma and the surrounding conductors. There are two types of solutions: (1) a solution that vanishes far from the plasma, the  $1/r^m$  solution, that is due to currents in the plasma region and (2) a solution that would become singular far from the plasma, the  $r^m$  solution, that is due to currents in the external conductors. Given  $\hat{n} \cdot \delta\vec{B} = \partial\phi/\partial r$  and  $\phi$  on a cylindrical surface, both solutions can be determined. The part of the solution due to the plasma currents, the  $1/r^m$  solution, is valid in the entire region outside of the plasma.

In principle, the response of external conductors could also be represented by a relation between  $\phi$  and  $\hat{n} \cdot \vec{\nabla}\phi$  on a surface. However, the external conductors present a more complicated problem than the plasma for two reasons. First, the time scale of the resistive wall mode is determined by the resistive time scales of the wall and other external conductors. This means that the tangential magnetic perturbation depends, not only on the present normal magnetic perturbation, but also on its values in the past in a relatively complicated way. In many cases of practical interest the plasma time scales are either very long or very short compared to the resistive time scales of the wall, which eliminates this complication. Second and more importantly, some of the external currents are actively controlled while others are reactive. Consequently an accurate determination of the currents in external conductors requires a code such as VALEN [5].

For perturbations that have a time scale significantly different from that of the plasma, the plasma response is completely described by a matrix that relates the expansion coefficients of the normal magnetic field,  $\hat{n} \cdot \delta\vec{B} = \hat{n} \cdot \vec{\nabla}\phi$ , and the potential  $\phi$  on the plasma surface in any set of orthogonal functions. However, it is more convenient to use the expansion coefficients of the plasma current potential  $\kappa_p$  instead of those of  $\phi$ . A current potential  $\kappa$  is the jump in the scalar potential for a magnetic field across a surface current,  $\kappa \equiv -[\phi]/\mu_0$ .

Two distinct current potentials can be defined using the functions  $\hat{n} \cdot \delta\vec{B}$  and  $\phi$  at the location of the unperturbed plasma surface,  $\vec{x}_p(\theta, \varphi)$ . One gives the magnetic field produced by the perturbed plasma currents in the region external to the plasma. This current potential is  $\kappa_p(\theta, \varphi) \equiv \mu_0(\phi_I - \phi)$ , where  $\phi_I$  is the vacuum solution, evaluated on the plasma boundary, in the region occupied by the plasma with the boundary condition  $\hat{n} \cdot \vec{\nabla}\phi_v = \hat{n} \cdot \delta\vec{B}$ . The second gives the magnetic field due to the external currents in the region interior to the plasma surface. That current potential  $\kappa_x = \mu_0(\phi - \phi_x)$ , where  $\phi_x$  is the vacuum solution in the exterior region.

The magnetic field due to a current potential on the plasma surface,  $\vec{x}_p(\theta, \varphi)$ , is

$$\delta\vec{B}(\vec{x}) = \frac{\mu_0}{4\pi} \oint \frac{\vec{K} \times \vec{R}}{R^3} da = \frac{\mu_0}{4\pi} \oint \left( \frac{3\vec{R}}{R^5} \vec{R} \cdot - \frac{1}{R^3} \right) \kappa d\vec{a}, \quad (1)$$

where the surface current is

$$\vec{K} = \frac{1}{|(\partial\vec{x}_p/\partial\theta) \times (\partial\vec{x}_p/\partial\varphi)|} \left( \frac{\partial\kappa}{\partial\varphi} \frac{\partial\vec{x}_p}{\partial\theta} - \frac{\partial\kappa}{\partial\theta} \frac{\partial\vec{x}_p}{\partial\varphi} \right), \quad (2)$$

the area element is  $da = |(\partial \vec{x}_p / \partial \theta) \times (\partial \vec{x}_p / \partial \varphi)| d\theta d\varphi$ , and  $\vec{R} \equiv \vec{x} - \vec{x}_p$ . The expression for  $\vec{K}$  is obtained from Ampere's law  $\mu_0 \vec{K} = \hat{n} \times [\delta \vec{B}] = \hat{n} \times \vec{\nabla}[\phi]$ , the definition  $\kappa \equiv -[\phi]/\mu_0$ , and the theory of general coordinates. The current potential  $\kappa$  has units of Amperes and is a magnetic dipole moment per unit area.

Equation (1) gives a linear relation between a current potential  $\kappa$  and the normal magnetic field on the plasma surface. This linear relation determines an inductance matrix  $\mathbf{L}$ . To define this matrix, let  $f_i(\theta, \varphi)$  be any set of functions that are orthogonal when integrated over the plasma surface,  $\oint f_i^* f_j da / A = \delta_{ij}$  where  $A \equiv \oint da$  is the area of the surface. The normal component of the magnetic field on the surface  $\vec{x}_p$  produced by the current potential  $\kappa$  can be expanded in the  $f_i$  as  $\hat{n} \cdot \delta \vec{B} = \sum_i \Phi_i f_i^*(\theta, \varphi) / A$ . The expansion coefficients, the  $\Phi_i$ , have units of magnetic flux. The current potential can be expanded in terms of the  $f_j$  as  $\kappa = \sum J_j^* f_j(\theta, \varphi)$ , where the expansion coefficients  $J_j^*$  have units of Amperes. The  $\mathbf{L}$  matrix, which is determined by Equation (1), gives  $\Phi_i = \sum L_{ij} J_j$  or  $\vec{\Phi} = \mathbf{L} \cdot \vec{J}$ . The matrix  $\mathbf{L}$  is always positive and Hermitian, and its square root can be calculated using the square root of its eigenvalues.

The two current potentials  $\kappa_p$  and  $\kappa_x$ , which were defined in terms of  $\phi$  and  $\hat{n} \cdot \vec{\nabla} \phi$  on the plasma surface, can also be expanded in the orthonormal functions  $f_i$ . The current potential that represents the perturbed plasma current is expanded as  $\kappa_p = \sum I_j^* f_j$ , which implies that the normal magnetic field at the location of the unperturbed plasma surface due to the perturbed plasma currents is  $\hat{n} \cdot \delta \vec{B}_p = \sum \Phi_i^{(p)} f_i^* / A$  with  $\vec{\Phi}^{(p)} = \mathbf{L} \cdot \vec{I}$ . Similarly, the current potential that represents the external magnetic field is expanded as  $\kappa_x = \sum J_j^* f_j$ , and the normal magnetic field at the location of the unperturbed plasma surface due to the external currents is  $\hat{n} \cdot \delta \vec{B}_x = \sum \Phi_i^{(x)} f_i^* / A$  with  $\vec{\Phi}^{(x)} = \mathbf{L} \cdot \vec{J}$ .

The normal magnetic field perturbation on the plasma surface has been separated uniquely into a part due to the perturbed plasma currents and a part due to the external currents,  $\hat{n} \cdot \delta \vec{B} = \hat{n} \cdot \delta \vec{B}_p + \hat{n} \cdot \delta \vec{B}_x$ . The flux expansion coefficients of  $\hat{n} \cdot \delta \vec{B}$  are  $\vec{\Phi} = \vec{\Phi}^{(p)} + \vec{\Phi}^{(x)}$ . Using  $\kappa_p$ , the Biot-Savart integral of Equation (1) determines the magnetic field due to the plasma currents,  $\delta \vec{B}_p$ , at any point  $\vec{x}$  outside of the plasma.

For a non-rotating plasma that obeys the constraints of ideal magnetohydrodynamics (MHD), one can use an MHD stability code, such as Alan Glasser's DCON, to find an inductance matrix  $\mathbf{\Lambda}$ , which is defined by  $\vec{\Phi} = \mathbf{\Lambda} \cdot \vec{J}$ . The  $\mathbf{\Lambda}$  matrix gives a complete description of the external magnetic response of the plasma. The energy required to perturb an ideal plasma is  $\delta W = \vec{J}^\dagger \cdot \vec{\Phi} / 2 = \vec{\Phi}^\dagger \cdot \mathbf{\Lambda}^{-1} \cdot \vec{\Phi} / 2$ , which is the  $\delta W$  of ideal MHD [11]. DCON

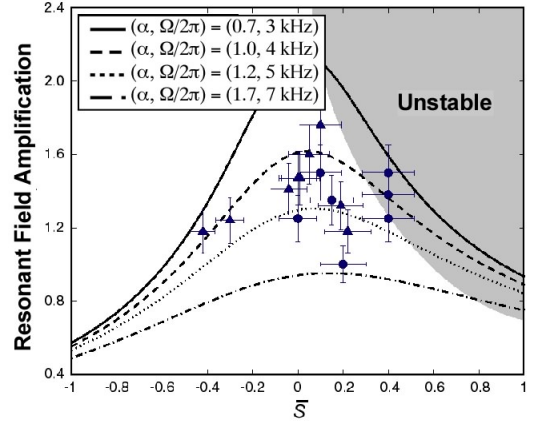


FIG. 3. Measurements of static-field resonant field amplification,  $A_{RWM}$ , as a function of stability parameter,  $\bar{s}$ . The observed amplification implies a large torque parameter,  $\bar{\alpha} \sim 1$ , associated with high dissipation.

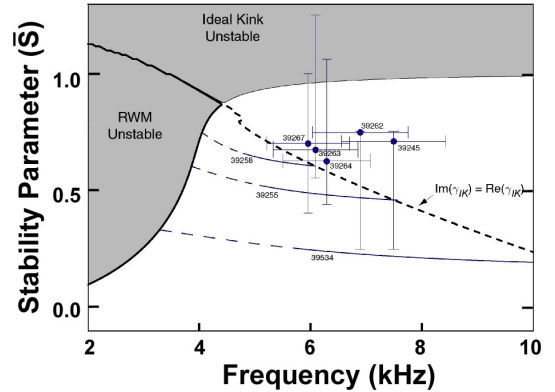


FIG. 4. Kink stability diagram for HBT-EP in the high dissipation regime.

provides a set of energies,  $\delta W$ , and their corresponding  $\hat{n} \cdot \delta \vec{B}$  distributions on the plasma surface, which is sufficient information to determine  $\mathbf{\Lambda}$  [13]. The required calculations to determine  $\mathbf{\Lambda}$  from DCON data have been carried out for a number of HBT-EP, DIII-D and JT-60SC cases [17]. Fig. 2 shows the amplitude of the first expansion function,  $f_1(\theta, \varphi)$ , computed over the unperturbed plasma surface for HBT-EP. It corresponds to the unstable plasma mode, as determined by DCON. The structure of this mode is kept unchanged by using the Gram-Schmidt orthonormalization process to construct expansion functions,  $f_i(\theta, \varphi)$ , from the normal magnetic field distribution on the plasma surface provided by DCON.

The external magnetic response of a plasma is completely characterized by the  $\mathbf{\Lambda}$  matrix whenever the time scales of the plasma are disparate from those of the resistive wall mode or other external perturbations. However, the physics of the response has a simpler characterization through the dimensionless stability matrix, which is defined by  $\mathbf{S} \equiv \mathbf{L}^{1/2} \cdot \mathbf{\Lambda}^{-1} \cdot \mathbf{L}^{1/2}$ . If a non-rotating plasma obeys the constraints of ideal MHD,  $\mathbf{S}$  is Hermitian. Its real eigenvalues are  $-s_j$ , the stability coefficients. The plasma amplifies an external perturbation if  $s_j > -1$  and reduces perturbations if  $s_j < -1$ . If at least one of the  $s_j$  is positive, the amplification is sufficiently great that the plasma is unstable. For a more general plasma model  $\mathbf{S}$  is not Hermitian, and its eigenvalues are complex numbers,  $-s_j + i\alpha_j$ . The imaginary part of the eigenvalue [13] gives the toroidal torque,  $T_\varphi$ , exerted on the plasma by the external conductors,  $T_\varphi = \oint (\partial \vec{x}_p / \partial \varphi) \cdot (\vec{K}_p \times \delta \vec{B}_x) da$ , which can also be written as  $T_\varphi = - \oint (\partial \kappa_p / \partial \varphi) \delta \vec{B}_x \cdot d\vec{a}$ .  $\vec{K}_p$  is the surface current obtained from the current potential  $\kappa_p$ , and the integral is over the plasma surface. Plasma rotation changes both the real and the imaginary parts of the eigenvalues of  $\mathbf{S}$ . In a simple plasma model, the changes in both are linear in the toroidal rotation frequency of a slowly rotating plasma, and slow rotation is stabilizing [13]. Unless the toroidal torque is small,  $|\alpha_j| \ll 1$ , the structure of a magnetic perturbation must be changed substantially from its ideal MHD form. If  $|\alpha_j| > 1$ , the plasma currents that produce the torque on the plasma strongly shield the external magnetic perturbation.

The simplest representation of plasma response for inclusion in a code like VALEN is the current potential of the plasma,  $\kappa_p$ , that arises from an arbitrary external normal field on the plasma surface,  $\hat{n} \cdot \delta \vec{B}_x$ . This is equivalent to giving the expansion coefficients of  $\kappa_p$ , the  $\vec{I}$ , in terms of the expansion coefficients of  $\hat{n} \cdot \delta \vec{B}_x$  on the plasma surface, the  $\vec{\Phi}^{(x)}$ . Simple matrix algebra implies  $\vec{I} = \mathbf{L}^{-1/2} \cdot (\mathbf{S}^{-1} - \mathbf{1}) \cdot \mathbf{L}^{-1/2} \cdot \vec{\Phi}^{(x)}$ . If an eigenvalue of the stability matrix,  $-s_j + i\alpha_j$ , is much smaller in absolute value than the other eigenvalues, then the associated eigenmode dominates the plasma response. Models based on the approximation of keeping only the term in  $\mathbf{S}$  with the smallest eigenvalue is called the

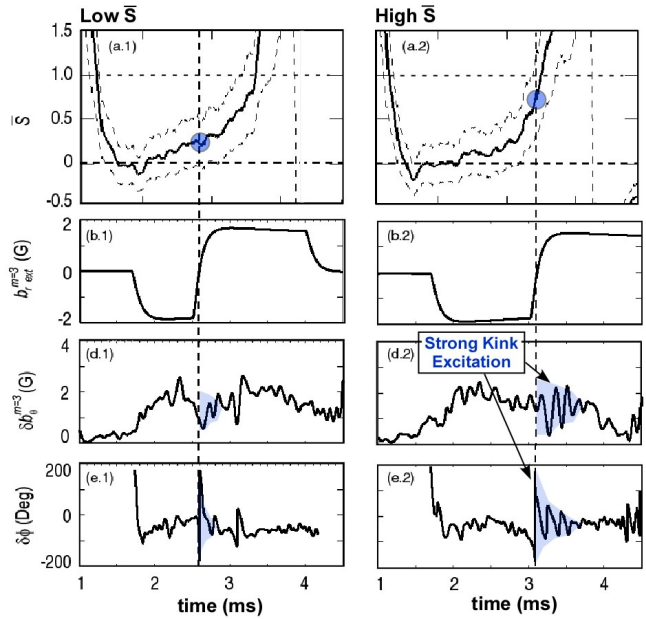


FIG. 5. The “single-mode” stability diagram for HBT-EP (top) showing rotation stabilization in the high-dissipation regime. Summary of “phase-flip” measurements (bottom) showing strong kink excitation at high  $s$ .



single-mode model. Within the single-mode model, it is relatively simple to empirically find the real and the imaginary parts of the eigenvalue, the  $s$  and the  $\alpha$ , that represent the plasma response to magnetic perturbations produced by external currents.

### 3. Measurement of Kink Mode Dynamics

RWM dynamics are studied experimentally as a function of kink stability and of plasma rotation by direct measurement of the plasma response to both quasi-static and rapid “phase-flip” changes in external resonant magnetic perturbations [10]. The plasma resonant response is characterized by an amplitude and phase that are directly related to the dominate complex eigenvalue,  $s + i\alpha$ . In order to compare measurement with theory, (i) the evolution of the plasma equilibrium is reconstructed from measurements and transport models of plasma current diffusion, (ii) the  $(m, n) = (3, 1)$  kink mode structure is computed by the DCON MHD, and (iii) VALEN is used to accurately compute the wall penetration rate for the resonant fields,  $\gamma_w \approx 5 \text{ ms}^{-1}$ , and the coupling coefficient,  $c \sim 0.17$ , between the segmented external conducting structures (Fig. 1) and the kink mode. Additionally, the effective natural toroidal rotation rate of the plasma and kink mode,  $\Omega$ , is obtained from the unperturbed rotation of MHD instabilities, a two-fluid force balance [18], and high-speed optical measurements of Doppler-shifted impurity lines [19].

The response to an externally-programmed resonant error field evolves in accord with the wall’s resistive diffusion equation,  $(d\psi_w/dt) + (\gamma_w/1-c)(\psi_w - \sqrt{c}\psi_a) = \gamma_w\psi_c$ , with the perturbed magnetic flux,  $\psi_c$ , being specified by it’s value at the conducting wall without plasma.  $\psi_a$  and  $\psi_w$  are, respectively, the perturbed fluxes at the plasma surface and at the wall, and these fluxes can be measured in HBT-EP. A dynamical equation relating the perturbed flux at the plasma surface to the resonant flux at the wall was derived by Fitzpatrick and Aydemir [15, 16],

$$\frac{1}{\gamma_{MHD}^2} \frac{d^2\psi_a}{dt^2} - \left( \frac{\bar{\alpha}}{\Omega} + \frac{2i\Omega}{\gamma_{MHD}^2} \right) \frac{d\psi_a}{dt} + \left( 1 - \bar{s} + i\bar{\alpha} - \Omega^2/\gamma_{MHD}^2 \right) \psi_a = \frac{\psi_w}{\sqrt{c}}. \quad (3)$$

The terms containing the ideal MHD growth rate,  $\gamma_{MHD}^{-2}$ , represent small corrections that can usually be ignored, and the eigenvalue,  $(\bar{s}, \bar{\alpha})$ , is normalized to the ideal wall stability limit,  $s_{crit} \equiv c/(1-c)$ . Eq. 3 was derived from reduced MHD assuming a dissipation rate,  $\nu_d$ , from anomalous perpendicular viscosity, but any linear dissipation rate [14] leads to a torque parameter that scales with dissipation as  $\bar{\alpha} = -\nu_d\Omega/\gamma_{MHD}^2$ .

The plasma response from Eq. 3 takes a simple form when the plasma is rotating slowly,  $\Omega/\gamma_w \ll 1$ , and near the no-wall limit,  $\bar{s} \sim 0$ . In this case, the flux ratio depends only upon the single-mode eigenvalue and the coupling coefficient,  $(\psi_a/\psi_w)^{-1} = \sqrt{c}(1 - \bar{s} + i\bar{\alpha})$ . The other case is appropriate to HBT-EP discharges that operate above the no-wall limit with the RWM stabilized by plasma rotation (Fig. 4). The torque parameter is significant,  $\bar{\alpha} \sim 1$ , and the perturbed magnetic flux at the plasma surface also depends upon the dynamics of the wall-stabilized kink found in Eq. 3.

Fig. 3 shows measurements of the amplitude of the amplification of resonant field errors,  $|A_{RWM}|$ , in the HBT-EP experiment [10]. The amplification peaks at marginal stability for the RWM; however, the degree of amplification,  $1 < |A_{RWM}| < 2$ , remains relatively small. When the phase and amplitude of the response is compared to Eq. 3, the measurements dictate the torque parameter to be relatively large,  $\bar{\alpha} \sim 1$ .

The resonant response to a rapid, step-change in  $\psi_c$  provides a nearly instantaneous method to measure the plasma dynamic response and approach to marginal stability

[10]. Fig. 5 illustrates these measurements by showing the evolution of two discharges prepared to approach marginal stability of the RWM. When rapid toroidal “phase-flips” are programmed in the resonant external field, the amplitude and phase of the dynamical plasma response changes depending on whether the rapid change occurred (earlier) in more stable or (later) in less stable plasma. A lengthening of the phase-realignment time marks the approach to marginal stability of the wall-stabilized kink mode. The phase-flip response serves as a test of models that simulate RWM dynamics in rotating plasma. Analysis of the measured response from many discharges are superimposed on the stability diagram in Fig. 4 allowing accurate determination of the normalized stability parameters,  $(\bar{s}, \bar{\alpha})$ . With these parameters, the time variations of the amplitude and phase response are consistent with the single mode theories associated with RWM stabilization.

#### 4. High-Speed Digital Mode Control

As described previously [6], active feedback control of the the RWM can be optimized by (i) reducing the mutual inductive coupling between the control and sensor coils, (ii) increasing the direct coupling of the control coils to the plasma surface, and (iii) reducing the inductive coupling between the sensor coils and the stabilizing wall. We refer to feedback control systems with these improvements as “optimized mode control”, and they are capable of stabilizing kink modes near the ideal wall stability limit,  $\bar{s} \approx 1$ .

Using the VALEN code, new control and sensor coils were designed and installed in HBT-EP in order to test mode control stabilization of rapidly-rotating, wall-stabilized kink modes. Fig. 1b illustrates the new coil system consisting of 20 “picture frame” control coils located in gaps in the segmented wall and 20 inside poloidal field sensors. The new feedback system improves performance relative to the previous “smart shell” configuration [3] by allowing greater bandwidth and a 10 fold increase in system gain.

In addition to newly-installed and optimized coils, we have designed and implemented a new high-speed digital feedback controller using multiple Xilinx II field-programmable gate array (FPGA) processors. The FPGA processors are packaged with 8 channels each of 16-bit analog-digital input and digital-analog output. The digital controller operates with a combined throughput of 64 Mbits/sec and provides a unique and powerful tool for the study of active feedback control of resistive wall modes.

The initial operation of the controller has been successful [20]. External kink modes have been suppressed, excited, and rotated in the HBT-EP tokamak. Several digital algorithms have been tested experimentally, and phase-accurate control over a wide bandwidth has been demonstrated. Using optimized magnetic sensors and control coils, the amplitude of wall stabilized kink mode have been suppressed for plasmas near the ideal wall limit. Fig. 6 illustrates feedback performance for two different high-gain transfer functions of the digital controller. For each control algorithm, the phase between the controlling flux

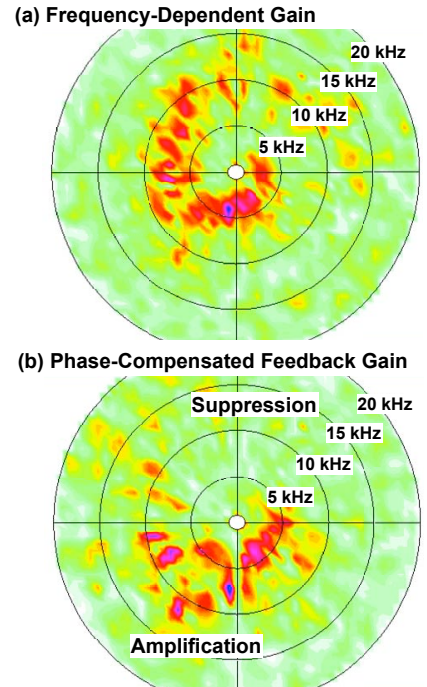


FIG. 6. Results of the application of active feedback control to unstable, rapidly rotating kink modes.

and the measured  $n = 1$  perturbed poloidal field was gradually incremented over 360 deg. As the control phase changes, the RWM can be suppressed or amplified, and the change in the rate of toroidal mode rotation illustrates the importance of proper compensation.

## 5. Summary

Fundamental theory, experimental observations, and modeling of the resistive wall mode (RWM) demonstrate how the complex interactions between a dominant resonant mode and the currents flowing in external conductors can be effectively modeled. The plasma response to both quasi-static and rapid, “phase-flip” perturbations were measured and compared with theory. For the class of discharges studied in HBT-EP, the torque parameter is large,  $\bar{\alpha} \sim 1$ , corresponding to the “high dissipation” regime for RWM dynamics. The time varying plasma response to a rapid step change in the external field error allows for a nearly instantaneous measurement of the plasma’s kink stability properties and approach to marginal stability. Additionally, the results from ongoing experiments include (i) investigations of the effectiveness of optimized mode control feedback to stabilize plasma near the ideal-wall stability limit, and (ii) the performance of high-speed digital algorithms and dedicated FPGA processors for plasma feedback control.

## Acknowledgement

We are pleased to acknowledge the technical expertise of N. Rivera, J. Andreello, and J. Moran and U. S. DOE Grants DE-FG02-86ER53222 and DE-FG02-03ER5496.

## References

- [1] A. D. Turnbull, *et al.*, Phys. Rev. Lett. 74, 718 (1995); C. Kessel, *et al.*, Phys. Rev. Lett. 72, 1212 (1994); and J. Menard, *et al.*, Nucl. Fusion 37, 595 (1997).
- [2] A. Garofalo, E. Strait, L. Johnson, *et al.*, Phys. Rev. Lett. 89, 235001 (2002).
- [3] C. Cates, M. Shilov, M. E. Mauel, *et al.*, Phys. Plasmas, 7, 3133 (2000).
- [4] M. Okabayashi, J. Bialek, M. S. Chance, *et al.*, Phys. Plasmas 8, 2071 (2001).
- [5] J. Bialek, A. Boozer, M. Mauel, G. Navratil, Phys. Plasmas 8, 2170 (2001).
- [6] D. Maurer, *et al.*, 19th IAEA Conf. Fusion Energy, IAEA-CN-94/TH/P3-13, (2002).
- [7] A. Boozer, Phys. Plasmas, 11, 110 (2004).
- [8] T. Ivers, E. Eisner, A. Garofalo, *et al.*, Phys. Plasmas, 3, 1926 (1996).
- [9] A. Garofalo, E. Eisner, T. Ivers, *et al.*, Nucl. Fusion 38, 1029 (1998).
- [10] M. Shilov, *et al.*, Phys. Plasmas, 11, 2573 (2004).
- [11] A. H. Boozer, Phys. Plasmas, 6, 3180 (1999).
- [12] A. H. Boozer, Phys. Rev. Lett., 86, 5059 (2001).
- [13] A. H. Boozer, Phys. Plasmas, 10, 1458 (2003).
- [14] M. S. Chu, *et al.*, Phys. Plasmas, 2, 2236 (1995).
- [15] R. Fitzpatrick and A. Y. Aydemir, Nuc. Fusion, 16, 11 (1996).
- [16] R. Fitzpatrick, Phys. Plasmas 9, 3459 (2002).
- [17] D. Maslovsky and A. H. Boozer, Phys. Plasmas, submitted for publication.
- [18] E. D. Taylor, *et al.*, Phys. Plasmas, 9, 3938 (2002).
- [19] S. F. Paul, *et al.*, Rev. Sci. Instr., 75, 4077 (2004).
- [20] A. Klien, *et al.*, submitted to Phys. Plasmas.